

NMR Measurement of the Alignment Tensor for a Polymer Melt under Strong Shearing Flow

M. L. Kilfoil[‡] and P. T. Callaghan^{*,†}

Institute of Fundamental Sciences-Physics, Massey University, Palmerston North, New Zealand, and Department of Physics and Physical Oceanography, Memorial University of Newfoundland, St. Johns, Newfoundland, Canada A1B 2X7

Received March 28, 2000

ABSTRACT: ²H NMR quadrupole interaction spectroscopy has been used to measure the deformation of a 610 kD PDMS melt under shear in a Couette cell. The signals were acquired from a perdeuterated benzene probe molecule, which provides a motionally averaged sampling of the entire segmental ensemble. Our Rheo-NMR method involves the use of a selective storage precursor pulse, which enables one to observe NMR spectra from preselected regions within the flow. We have measured the dependence on the shear rate of the S_{XX} (velocity) and S_{YY} (velocity gradient) elements of the segmental alignment tensor as well as the angular dependence of the deuterium quadrupole splitting at a fixed shear rate. The results agree well with Doi–Edwards theory and return a value for the tube disengagement time of 310 ms.

Introduction

When a random coil polymer melt is subjected to shear, the polymer chain suffers a biaxial deformation in which the principal axis of extension has a preferred orientation with respect to the hydrodynamic velocity direction. The geometry is as indicated in Figure 1. The deformation may be usefully described by means of the averaged segmental alignment tensor,

$$S_{\alpha\beta}(t) = \left\langle \int_0^L ds u_\alpha(s,t) u_\beta(s,t) - \frac{1}{3} \delta_{\alpha\beta} \right\rangle \quad (1)$$

where $\langle \dots \rangle$ represents the ensemble average and the integral is taken over the curvilinear path of \mathbf{s} chain segments along the chain length L . In the Doi–Edwards formulation of entangled polymer dynamics,^{1,2} the stress tensor $\sigma_{\alpha\beta}$ is shown to be directly proportional to the average alignment tensor $S_{\alpha\beta}$. Where polymer segments are aligned so that $S_{\alpha\beta}$ is non-zero, other physical properties will be anisotropic as well. In particular, the dielectric properties that determine the material refractive index will be affected, leading to the optical anisotropy known as birefringence. The correspondence of the stress tensor and the anisotropic part of the refractive index tensor is known as the “stress-optical law” and is expressed by the relation

$$n_{\alpha\beta} = C \sigma_{\alpha\beta} \quad (2)$$

C is known as the stress-optical coefficient.^{2,3}

Birefringence measurements may be used⁴ to investigate the segmental alignment tensor and so give some insight regarding the deformation depicted in Figure 1. If incident plane polarized light has its polarization axis parallel to the extension axis, a unique refractive index is observed. In this case extinction will occur between polarizers crossed at some angle χ , generally called the extinction angle. Maximum birefringence effects will be apparent if the polarization axis is incident at 45° to

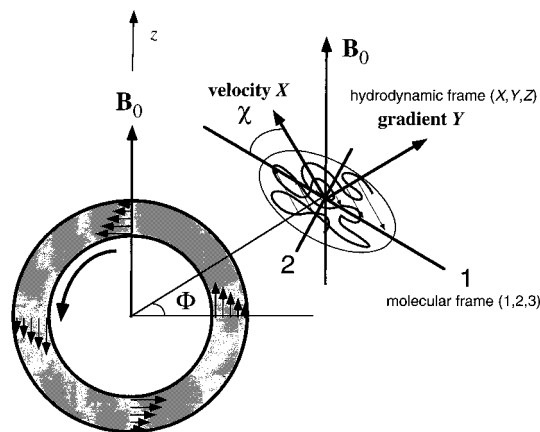


Figure 1. Schematic diagram of a “horizontal Couette cell” in which the vorticity axis is aligned transverse to the magnetic field. The angle between the local velocity direction and the magnetic field is given by Φ . The angle between the principal axis of the molecular (1,2,3) frame and the velocity axis, X , is the so-called extinction angle, χ .

the extension axis and measurements of n_{\perp} and n_{\parallel} for such an arrangement may be used to investigate $S_{\alpha\beta}$.

The measurement of polymer deformation by optical methods relies on some underlying assumptions, for example, the identity of the macroscopic and microscopic polarizability tensor and the dominance of intrinsic birefringence over form birefringence. In the present article we report on an entirely new method of measuring polymer deformation under shear in which the orientation of bond vectors is determined through nuclear spin interactions. We use nuclear magnetic resonance to determine the strength of the electric quadrupole interaction of deuterons, a quantity which depends in a very simple manner upon the relative orientation of the electric field gradient axis (the bond axis) and the polarizing magnetic field used to produce the nuclear Zeeman effect. In our experiments reported here, the deuteron is present in a small probe molecule that rapidly samples the mean alignment of the host polymer. Because of the use of such an indirect probe, the measurement of alignment is not absolute and, like

* To whom correspondence should be addressed.

[†] Massey University.

[‡] Memorial University of Newfoundland.

the birefringence method, relies on an equivalent to the stress-optical coefficient. However, the measurement of "extinction" is absolute and we are able to investigate the shear-rate dependence of the interaction, thus testing the predictions of Doi–Edwards theory.

Theory

Measurement of Segmental Alignment by NMR.

A spin-one deuterium nucleus will experience an electric quadrupole interaction between the nuclear quadrupole moment and the surrounding electric field gradient. This interaction is experienced in the presence of an overwhelmingly larger Zeeman interaction between the magnetic dipole moment and the polarizing magnetic field \mathbf{B}_0 and, as a consequence, is observed as a first-order perturbation projected along the spin quantization axis defined by the static magnetic field. This direction, normally labeled the z axis, is to be distinguished from the hydrodynamic vorticity direction, Z . For an axially symmetric electric field gradient, as is typically found in a carbon–deuterium bond, the quadrupole interaction takes the form

$$H_Q = \frac{3eV_{zz}Q}{4I(2I-1)} P_2(\cos \theta) (3I_z^2 - I^2) \quad (3)$$

Here, θ is the angle between the field gradient axis and the polarizing magnetic field, V_{zz} is the electric field gradient strength, Q is the nuclear quadrupole moment, and I is the nuclear spin quantum number. The effect of H_Q is to split the deuterium resonance into a doublet separated in frequency by $(3/2 eV_{zz}Q/h) P_2(\cos \theta)$. The quadrupole interaction strength $3/2 eV_{zz}Q/h$ is usually on the order of 100 kHz in partially ordered systems. The angular dependence arising from the second-rank Legendre polynomial, $P_2(\cos \theta)$, makes it possible to use the quadrupole splitting to determine mean bond orientation.

In simple isotropic liquids, molecular tumbling causes θ and hence H_Q to fluctuate. Provided that this motion is more rapid than the quadrupolar interaction strength, a condition which is true for all but the most viscous liquids, the quadrupolar Hamiltonian is averaged to zero. In anisotropic liquids, the motional averaging is incomplete. Suppose there exists a local director, inclined at angle α to the magnetic field \mathbf{B}_0 , which is fixed in space or which fluctuates slowly by comparison with the quadrupolar frequency. The orientation (θ, ϕ) of the electric field gradient (bond) axis with respect to \mathbf{B}_0 can then be decomposed into $(\theta_\alpha, \phi_\alpha)$ describing the bond axis with respect to the director, and α . Let us for the moment assume that distribution of $(\theta_\alpha, \phi_\alpha)$ with respect to the axis labeled by α is independent of the particular orientation of that axis. The significance of this assumption will be discussed in the next section. Meanwhile, we note that the spherical harmonic addition theorem may be used to factorize as follows,⁵

$$\overline{P_2(\cos \theta)} = \overline{P_2(\cos \theta_\alpha)} P_2(\cos \alpha) \quad (4)$$

$\overline{P_2(\cos \theta_\alpha)}$ thus defines a local order parameter that scales the quadrupole interaction strength.

Here, we consider the case of a small benzene probe molecule that is placed as a dilute species near a polymer segment whose orientation \mathbf{u} defines the local director. The tumbling probe molecule will undergo steric interactions with that segment and experience an

anisotropic mean orientation. The probe will thus exhibit a scaled down quadrupole splitting associated with that local site via a "pseudo-nematic" interaction.⁶ This interaction is akin to the local anisotropic steric interaction experienced by small probe molecules placed in a nematic liquid crystalline environment.⁷ On average, the probe molecule samples an ensemble average value for $P_2(\cos \alpha)$ as it diffuses over the molecular dimensions. For typical small molecules the diffusion time to cross the molecular length scale is certainly sufficiently short to ensure that motional averaging occurs in the sampling of the distribution of \mathbf{u} vectors. The ensemble average of $P_2(\cos \alpha)$ is identically $S_{zz} = \langle \int_0^L ds u_z(s) u_z(s) - 1/3 \rangle$, and the quadrupole splitting may be written

$$\Delta\nu = \left(\frac{3}{2} \frac{eV_{zz}Q}{h} \right) \overline{P_2(\cos \theta_\alpha)} S_{zz} \quad (5)$$

In the Doi–Edwards description of the alignment tensor $S_{\alpha\beta}$, the relevant axis system is the hydrodynamic frame described respectively by the velocity (X), velocity gradient (Y), and vorticity (Z) axes. Thus, to relate Doi–Edwards theory to the case of the NMR quadrupole interaction experiment, it is necessary to transform this tensor into the frame of the magnetic field, i.e.,

$$\mathbf{R}(\Theta, \Phi) \begin{pmatrix} S_{XX} & S_{XY} & 0 \\ S_{XY} & S_{YY} & 0 \\ 0 & 0 & S_{ZZ} \end{pmatrix} \mathbf{R}^{-1}(\Theta, \Phi) \quad (6)$$

where the polar angle Θ defines the direction of the vorticity axis Z relative to \mathbf{B}_0 and the azimuth Φ defines the orientations of X and Y . We are concerned with an experiment in which the vorticity axis is situated normal to \mathbf{B}_0 and the projection along \mathbf{B}_0 is in the X – Y (velocity–velocity gradient) plane. We write

$$S_{ZZ} = S_{XX} \cos^2 \Phi - 2S_{XY} \sin \Phi \cos \Phi + S_{YY} \sin^2 \Phi \quad (7)$$

for the diagonal tensor element representing the interaction strength measured in the NMR experiment. Note that this expression reduces to $P_2(\cos \Phi) S_{XX}$ for $S_{XY} = 0$, $S_{YY} = S_{ZZ} = -1/2 S_{XX}$, that is, when the deformation is uniaxial.

The Doi–Edwards Model for Segmental Alignment under Steady Shear. The standard description for polymer deformation under shear is the tube-reptation model of Doi and Edwards,¹ parametrized by the tube disengagement time τ_d and the tube diameter a . τ_d is the dominant relaxation time for the internal dynamics of the polymer; in this model it is the time for the polymer chain to leave the deformed tube by reptation. By solving the diffusion equation in the tube, Doi and Edwards show that the equilibrium deformation is given by

$$S_{\alpha\beta}(s, t) = \int_{-\infty}^t dt' \left(\frac{\partial}{\partial t'} \psi(s, t-t') \right) U_{\alpha\beta}^{IA}(\mathbf{E}(t, t')) \quad (8)$$

$\psi(s, t)$ is the probability that the chain segment s is in the deformed tube at time t and U is the independent alignment approximation for the tube orientation distribution. In the independent alignment approximation the segments deform affinely. The stress tensor is written

$$\sigma_{\alpha\beta}(t) = G_e \frac{1}{L} \int_{-L/2}^{L/2} ds S_{\alpha\beta}(s, t) \quad (9)$$

where $G_e = 3k_B Tcb^2/a^2$, b is the Kuhn segment size, and c is the segment concentration.

For the reptation model it is convenient to set $\psi(t) = 1$ for $t < \tau_d$ and 0 for $t > \tau_d$. $\partial/\partial t \psi(t - t')$ reduces to $\delta(t - (t - \tau_d))$ and the relevant deformation, \mathbf{E} , is simply that which occurs for shear rate over the duration, τ_d . In the case of steady shearing at rate $\dot{\gamma}$ that deformation is $\dot{\gamma}\tau_d$ so that

$$\sigma_{\alpha\beta}(\dot{\gamma}) \approx G_e S_{\alpha\beta}(\dot{\gamma}) = G_e U_{\alpha\beta}^A(\dot{\gamma}\tau_d) \quad (10)$$

However, here we have evaluated eq 8 using the exact reptation expression for $\psi(t)$, namely, $\sum_{p \text{ odd}} (8/\pi^2 p^2) \exp(-p^2 t/\tau_d)$. Figure 2a shows the relevant elements of the $S_{\alpha\beta}$ tensor, where X , Y , and Z are the hydrodynamic velocity, gradient, and vorticity directions. Figure 2b shows the shear-rate dependence of the extinction angle χ . In terms of the stress tensor, χ is the alignment angle that the principal axes of $\sigma_{\alpha\beta}$ make with the velocity direction X .

Nonlinear viscoelastic behavior becomes important at moderate shear rates in polymers having large τ_d values. Shear thinning occurs once the Deborah number $\dot{\gamma}\tau_d$ exceeds unity. In fact, the Doi-Edwards model states that for shear rates in excess of $1/\tau_d$, the rate of decrease of viscosity is so sharp that the shear stress actually declines, thus predicting unstable flow in shear regimes where, experimentally, only stable flow has been observed. Various refinements to the Doi-Edwards model modify the flow curve, and in particular the severity of the stress decline beyond $\dot{\gamma}\tau_d \sim 1$. These include the effects of contour length fluctuations,^{8,9} nonaffine tube deformation,¹⁰ and convected constraint release.¹¹ In the present analysis we shall use the unrefined Doi-Edwards model to compare measured and calculated segmental alignment elements.

At this point we revisit the assumption of independence of the $(\theta_\alpha, \phi_\alpha)$ distribution on α . For the entangled polymer, consider shear deformation at a strain rate on the order of or faster than the tube disengagement rate τ_d^{-1} but slower than the Rouse rate τ_R^{-1} . The orientation distribution of tube segments becomes anisotropic but the tube step length and the dynamics of the segmental motion at length scales smaller than a tube step are unperturbed. Consequently, we may take α to represent the tube step vector with the $(\theta_\alpha, \phi_\alpha)$ distribution common to each such vector, thus underpinning the assumptions behind eq 4.

Experimental Section

The polymer sample studied in this work is high molecular weight ($M_w = 610$ kD) poly(dimethylsiloxane) (PDMS), $M_w/M_n = 2.0$ (as measured by GPC), obtained from Polysciences (Warrington, PA). M_0 , the molecular weight per monomer, is 74, and the molecular weight between chain entanglements M_e is 10^4 for this PDMS melt.¹² In this was dissolved approximately 10% w/w per-deuterated benzene (Aldrich, Steinheim, Germany). Rheo-NMR measurements were carried out at a deuteron frequency of 42 MHz in an AMX300 spectrometer, using a specially constructed shear cell. Figure 3 shows our Rheo-NMR apparatus. It comprises a Couette cell made of a machinable glass (MACOR) inner cylinder of outer diameter 5 mm and a glass outer cylinder of inner diameter 6 mm. The poly(dimethylsiloxane) is enclosed in the 0.5-mm gap between these cylinders. Surrounding the cell is an rf coil tuned for deuterium (^2H). This assembly fits inside a set of

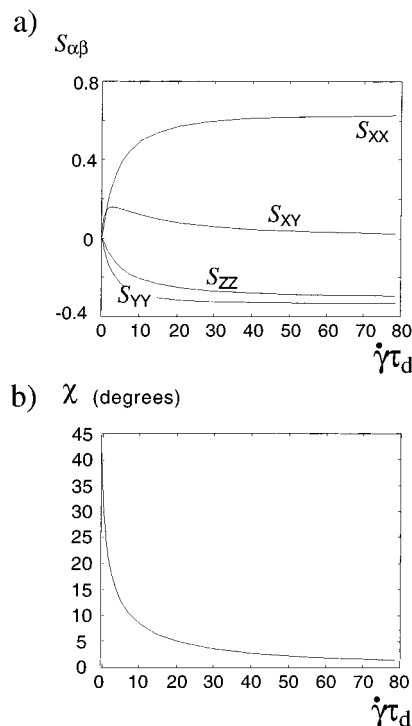


Figure 2. (a) Elements of the alignment tensor, $S_{\alpha\beta}$, and (b) the extinction angle χ , as a function of the reduced shear rate, $\dot{\gamma}\tau_d$, according to the Doi-Edwards model.

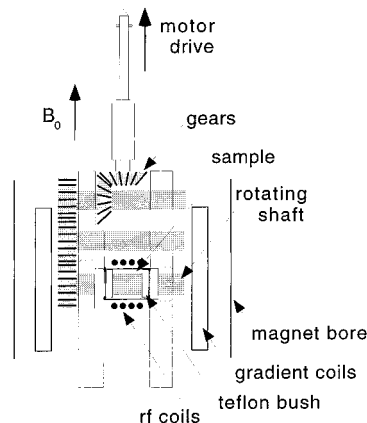


Figure 3. Mechanical arrangement of the horizontal Couette cell used in this work. The gear mechanism is driven by a vertical shaft down the magnet bore.

gradient coils and the entire probe is inserted in a 7 T superconducting magnet such that the vorticity axis (the cylinder axis) is normal to the polarizing field. The inner cylinder is rotated through a gear stage above the cell that is connected via a drive shaft running up the bore of the magnet to a gearbox and stepper motor mounted above.

Standard NMR microimaging¹³ is used to view the PDMS in the Couette gap, to image the velocity distribution across the gap (Figure 4a), or to excite a desired region of the sample for spectroscopy experiments (Figure 4b) during steady-state shear. This latter image shows that in one case the selected region has the velocity direction coincident with the polarizing field \mathbf{B}_0 , while in the other, the velocity gradient (shear axis) is parallel to \mathbf{B}_0 . The selective excitation pulse sequence used has been specially devised to minimize exposure of selected nuclear spins to any relaxation, so that high-quality NMR spectroscopy can be performed in the desired region. We describe this method in another article;¹⁴ however, the essential details are shown in Figure 5. The technique employs a selective precursor pulse sandwich that destroys magnetization outside the desired region but stores along the z -axis for

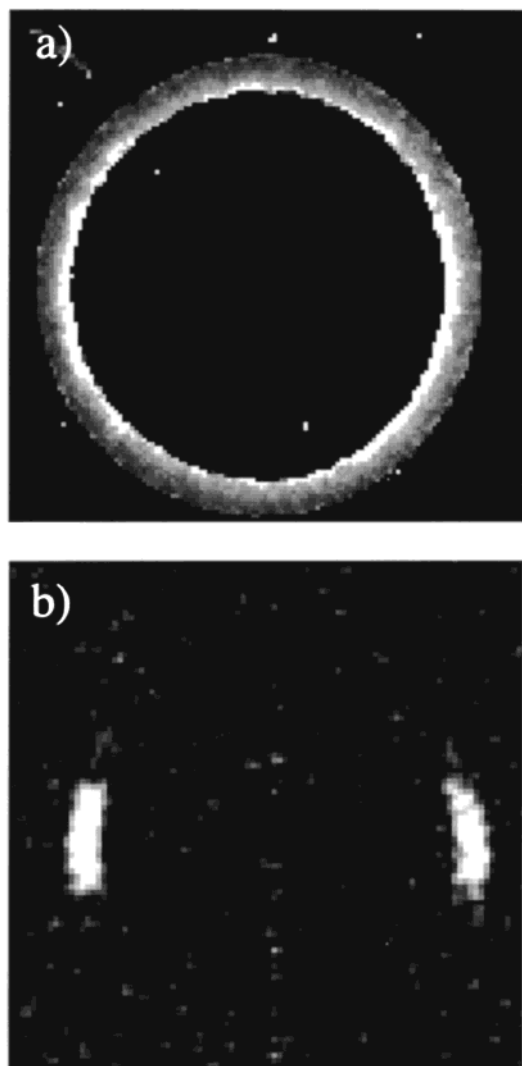


Figure 4. (a) Speed map showing the shear across the Couette cell. This map was reconstructed from two NMR images that had been respectively encoded for velocity components in the x and z direction. Details of the velocity encoding method can be found in chapter 9 of ref 13. (b) NMR image obtained following selective storage of magnetization from a desired region of the Couette cell. The image shows the region of sample that contributes to spectroscopy experiments when $\Phi = 0$ (velocity direction parallel to \mathbf{B}_0).

later recall the magnetization from the region of interest. Using the pulse sequence of Figure 5a, this magnetization can be used to obtain a confirmatory image (see Figure 4b), or using the sequence shown in Figure 5b, it may be recalled for NMR spectroscopy. Our spectroscopic method involves a Hahn echo that refocuses all unwanted Zeeman interactions arising from susceptibility inhomogeneity and leaves undisturbed the desired but weak quadrupolar precession. Fourier transformation of the echo amplitude with respect to the evolution dimension t_1 results in the quadrupolar spectrum. With this method we are able to resolve and measure quadrupole splittings of a few Hz.

Results and Discussion

Figure 6 shows a series of ^2H spectra obtained using the two-dimensional quadrupole spectroscopy sequence shown in Figure 5b. These spectra were acquired for a range of shear rates as indicated, in the region of the Couette cell in which the velocity axis X is aligned with the magnetic field direction. The shear rates were calculated from the known inner cylinder rotation speed

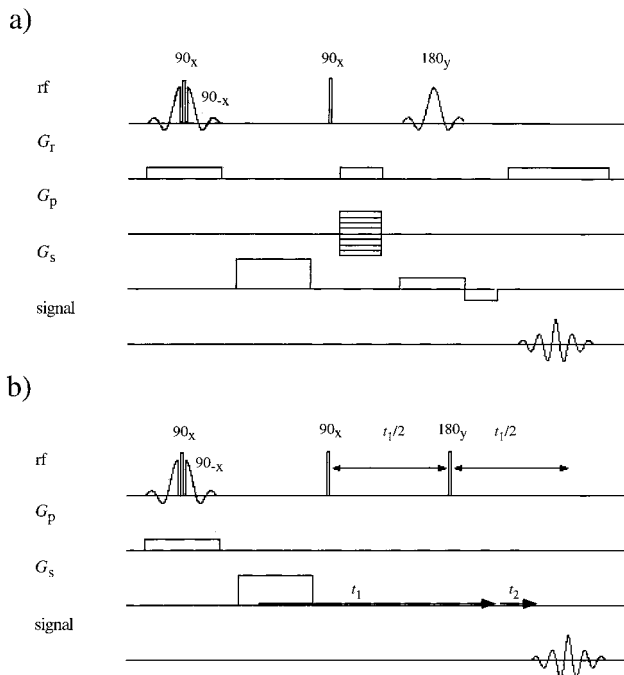


Figure 5. Rf and gradient pulse sequence used to obtain images and spectra from selected regions of the sample. The section of the pulse sequence before the dashed line is the selective storage segment that destroys all unwanted magnetization and stores the desired magnetization along the z -axis for later recall, in (a) for subsequent imaging and in (b) for subsequent NMR spectroscopy. The spectroscopic pulse sequence shown in (b) uses a spin-echo to refocus unwanted Zeeman interactions while retaining the desired evolution, over the t_1 interval, under the quadrupole Hamiltonian.

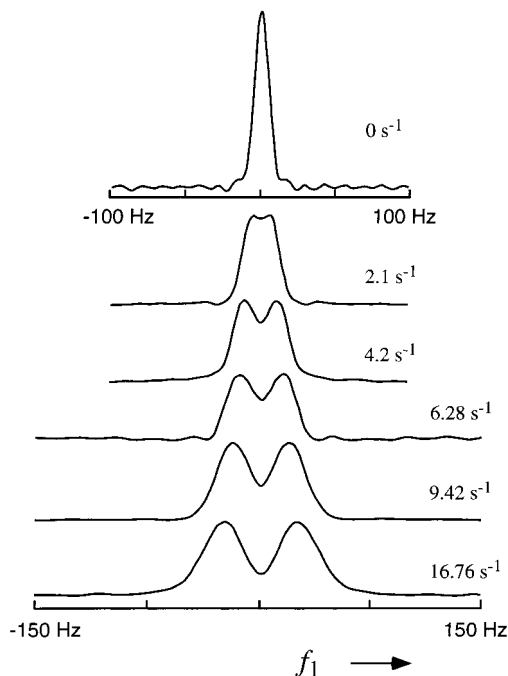


Figure 6. Examples of deuterium NMR spectra obtained by Fourier transforming the signal evolution in the t_1 domain. The splitting arises from the electric quadrupole interaction and is a measure of the ensemble-averaged local order.

and confirmed by velocity microimaging. Note the increasing width of the peaks as the shear rate increases, an effect which we attribute to slight heterogeneity in the shear field, thus leading to a distribution of splittings whose width is proportional to the average

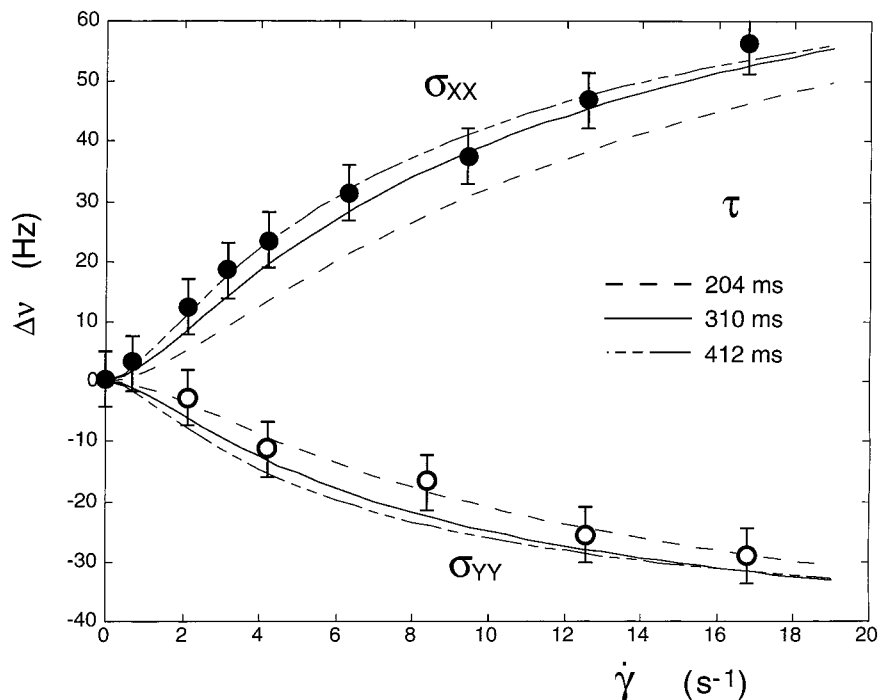


Figure 7. Quadrupole splittings, $\Delta\nu$, obtained from the spectra as shown in Figure 6, for a selected region of the horizontal Couette cell in which the velocity direction (solid circles) and gradient direction (open circles) are respectively parallel to the magnetic field. The lines are fits using the Doi–Edwards model in which the absolute splitting (vertical axis) is scaled to yield the pseudonematic order parameter and the horizontal axis is scaled to yield the tube disengagement time, τ_d . The best compromise fit corresponds to $\tau_d = 310$ ms.

shear rate. A corresponding set of data was acquired for the Couette cell region in which the velocity gradient direction Y was coincident with the field axis. Figure 7 shows the dependence of these splittings on shear rate. On the same graph we plot the corresponding Doi–Edwards alignment tensor curves (eq 10) in which the effective quadrupole interaction strength is scaled to match the absolute alignment and the tube disengagement time is adjusted to match the reduced shear rate $\dot{\gamma}\tau_d$. The fit to the two curves is quite good and any remaining discrepancy from the Doi–Edwards theory may be due to the chain length polydispersity or to the small nonuniformity in the shear rate. The best overall fit yields a tube disengagement time of 310 ms and a pseudonematic order parameter, $P_2(\cos\theta_0)$, of 4.74×10^{-4} . We note that the tube disengagement time obtained by this method agrees well with that for un-cross-linked polymers of high molecular weight, calculated according to¹⁵

$$\tau_d = \frac{a^2 \zeta_0 M_w^3}{M_e M_0^2 \pi^2 k_B T} \quad (11)$$

Using the literature values¹⁵ for the tube diameter a and the monomeric frictional coefficient ζ_0 , we calculate $\tau_d = 350$ ms.

We have also carried out this experiment at a fixed shear rate ($\dot{\gamma}\tau_d = 3.9$), varying the angle Φ between the velocity direction X and the magnetic field direction through a number of prescribed angles. This was achieved by changing the orientation of the magnetic field gradient used in the precursor selective storage pulse. The angular dependence of the splitting is shown in Figure 8, along with the Doi–Edwards curve calculated using eq 7. Again, the agreement is excellent. At this particular value of the reduced shear rate, the

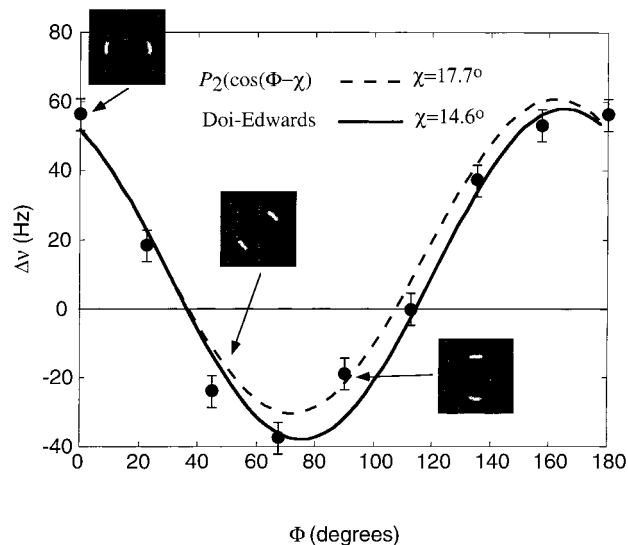


Figure 8. Quadrupole splittings, $\Delta\nu$, versus orientation angle, Φ , at a fixed Deborah number of $\dot{\gamma}\tau_d = 3.9$. 0° corresponds to the velocity axis aligned with \mathbf{B}_0 and 90° to the gradient axis aligned with \mathbf{B}_0 . The solid line shows the predictions of the Doi–Edwards model, with the angular dependence as given by eq 7. The dashed line corresponds to a simple uniaxial transformation ($P_2(\cos(\Phi-\chi))$). χ is the corresponding extinction angle in each case. The images show the selected regions used to obtain $\Phi = 0^\circ, 45^\circ, \text{ and } 90^\circ$.

extinction angle, χ , is predicted to be 14.6° from the results in Figure 7. To gain some intuitive insight regarding the orientation of the polymer in the flow, we have shown plotted in Figure 8 the theoretical curve for $P_2(\cos(\Phi-\chi))$ with χ adjusted to give the best fit ($\chi = 17.7^\circ$). Such a theoretical curve is naively based on the assumption of an axially symmetric polymer deformation, whereas the Doi–Edwards formulation predicts a non-zero second normal stress difference, $\sigma_{yy} - \sigma_{zz}$.

The poorer fit to the data given by this naive model provides independent confirmation of the biaxial nature of the deformation and further support for the Doi–Edwards description.

One defect of the present approach involves the need to use an indirect probe of the segmental order and the possibility that the benzene diluent may plasticize the polymer and significantly alter its dynamical behavior. To check this point, we have carried out flow curve measurements on 610 kD PDMS both with and without the 10% benzene and find no significant difference in the behavior. A different approach to direct measurement of the alignment tensor would be to use a perdeuterated polymer. Apart from the difficulty in obtaining high molecular mass PDMS, there exists an additional complication in that the nature of the motional averaging is quite different when signals are acquired from deuterons attached to the polymer chain. Now the characteristic time over which a given deuteron-labeled segment is able to sample the entire ensemble of possible orientations, \mathbf{u} , is given by the tube disengagement time (≈ 10 ms) rather than the time for a small probe molecule to diffuse over the chain dimensions (≈ 0.1 ms). Consequently, the averaged interaction will arise from a subensemble of orientations and the overall ^2H NMR spectrum will reflect an inhomogeneous distribution of such subensemble spectra. The distribution of subensemble effective directors will lead to somewhat different average quadrupolar splittings than those predicted by the Doi–Edwards curves of Figure 2, although there should exist significant differences in the nature of the quadrupole spectra observed when different sample orientations Φ are chosen.

In principle, it is possible to use the proton dipolar interaction to gain similar information regarding chain segment alignment, and such experiments avoid the need to isotopically label. The proton spectrum may be complicated by the influence of scalar spin–spin interactions (although these are absent in the case of PDMS), by the role of long-range dipolar couplings that are superposed on the desired, local two-spin couplings, and by the complexities of motional averaging discussed in the previous paragraph. A recent study of weak dipolar spectral broadening in sheared PDMS has however revealed a significant alignment effect and one which is dependent on the selection angle Φ .¹⁶

Conclusion

We have shown here that deuterium NMR spectroscopy can provide useful insight regarding the deformation of polymers under shear. Our results obtained from 610 kD PDMS, up to a Deborah number in excess of 5, are consistent with the classical Doi–Edwards description and yield a value for the tube disengagement time, which is consistent with other measurements for this particular polymer. The use of an isotopically labelled small-molecule probe has the advantage of experimental simplicity and the nature of the motional averaging achieved means the full segmental ensemble average is returned in the NMR spectrum, albeit with an unknown scaling factor for the pseudonematic interaction. This scaling factor is however no different in principle from the stress-optical coefficient required in birefringence studies. Our Rheo-NMR method has significant advantages in that it avoids the need for sample transparency, is not affected by unwanted scattering

impurities, voids, or irregular surfaces, and provides a local, microscopic description for which the known spin Hamiltonian gives the basis for an exact theory.

By changing the nature of the labeled probe, it may be possible to gain additional information. For example, site-specific deuteron labeling on the polymer could return the alignment tensor, $S_{\alpha\beta}(s)$, corresponding to different points along the polymer chain. Where a diluent probe molecule is used, different motional averaging regimes could be accessed by tuning the molecular diffusion coefficient. It is possible, in principle, to study deformation at specific molecular sites within blends, and by use of a probe molecule that can partition between different regions of the sample, it may be possible to study translational ordering. In a recent experiment, anomalous alignment effects have been observed when the probe diluent is a small oligomer, an effect which was attributed to weak smectic ordering.¹⁶

Other NMR isotopic labels are possible which access orientational order. In particular, ^{13}C has a large anisotropic chemical shift whose angular dependence when measured in the \mathbf{B}_0 field can provide information regarding the distribution of local director alignment. While ^{13}C labeling is expensive, abundant sites do exist in most polymers of interest and this spin probe could prove effective in the study of model molecular systems.

Finally, we note that for $\dot{\gamma}\tau_d \gg 1$ the Doi–Edwards picture may hold longer. We hope to extend our Rheo-NMR observations further into this regime to investigate possible deviations.

Acknowledgment. M.L.K. acknowledges financial support from the National Research Council of Canada while P.T.C. is grateful to the New Zealand Foundation for Research, Science and Technology and to the Royal Society of New Zealand respectively for funding support under the Public Good Science Fund and the Marsden Fund. The authors also acknowledge the assistance of Ryan Cormier in carrying out our flow curve measurements on PDMS samples.

References and Notes

- (1) Doi, M.; Edwards, S. F. *J. Chem. Soc., Faraday Trans. 2* **1978**, *74*, 1802 and 1818.
- (2) Doi, M.; Edwards, S. F. *The Theory of Polymer Dynamics*; Oxford University Press: Oxford, England, 1986.
- (3) Janeshitz-Kriegl, H. *Polymer Melt Rheology and Flow Birefringence*; Springer: New York, 1983.
- (4) Fuller, G. G. *Optical Rheometry of Complex Fluids*; Oxford University Press: New York, 1995.
- (5) Abragam, A. *The Principles of Nuclear Magnetism*; Oxford University Press: Oxford, England, 1961.
- (6) Deloche, B.; Samulski, E. T. *Macromolecules* **1981**, *14*, 575.
- (7) Burnell, E. E.; de Lange, C. A. *Chem. Rev.* **1998**, *98*, 2359.
- (8) Doi, M. *J. Polym. Sci. Lett.* **1981**, *19*, 265.
- (9) Rubinstein, M.; Panyukov, S. *Macromolecules* **1997**, *30*, 8036.
- (10) Marrucci, G. *J. Polym. Sci. Phys.* **1985**, *23*, 159.
- (11) Marrucci, G.; Ianniruberto, G. *J. Non-Newt. Fluid Mech.* **1999**, *82*, 275.
- (12) Callaghan, P. T.; Samulski, E. T. *Macromolecules* **1998**, *31*, 3693.
- (13) Callaghan, P. T. *Principles of Nuclear Magnetic Resonance Microscopy*; Oxford University Press: New York, 1991.
- (14) Kilfoil, M. L.; Callaghan, P. T. (in preparation).
- (15) Ferry, J. D. *Viscoelastic Properties of Polymers*, 3rd ed.; Wiley: New York, 1980.
- (16) Callaghan, P. T.; Kilfoil, M. L.; Samulski, E. T. *Phys. Rev. Lett.* **1998**, *81*, 4524.